Desalination and Water Treatment
www.deswater.com

doi: 10.5004/dwt.2023.29713

300 (2023) 158–166
July

Electrochemical oxidation of methyl blue dye using stainless steel rotating cylinder anode

Anas Bdiwi Salman[a,*], Safa Nabeel Abdulqahar[b]

[a]*Department of Chemical Engineering, Al-Muthanna University, Samawah, Iraq, email: dr.anas.bdiwi@mu.edu.iq*
[b]*Department of Chemical Engineering, Baghdad University, Baghdad, Iraq, email: safanabeel.abdulqahar@yahoo.com*

Received 31 January 2023; Accepted 17 June 2023

ABSTRACT

Several methods have been used for wastewater processing. Electrochemical oxidation is considered a potent technique for removing dyes from wastewater. In this study, methyl blue (MB) dye was successfully removed from contaminated wastewater using a stainless-steel rotating cylinder, and five factors were studied, including NaCl concentration, applied current, MB concentration, rotating cylinder speed and time. The response surface methodology with rotatable central composite design and half factorial method was used for the experimental design of this work and for deriving the mathematical model as well as the optimum conditions for this investigation, which included 95.0455 mg/L MB, 230 mA applied current, a rotation rate of 35 rpm, and 0.225 mg/L NaCl and 37.44 min time of reaction.

Keywords: Methyl blue; Electrochemical oxidation; Rotating cylinder; Response surface methodology

1. Introduction

Wastewater contaminated with organic textile dyes poses a real challenge to the environment due to the large amounts of stable coloured water formed from textile industries [1–3]. Synthetic dyes are significantly harmful substances for the environment, since they are non-biodegradable and cause odour, discolouration, oxygen deficiency and bioaccumulation [4,5].

Several methods have been investigated for organic textile dye removal, some of which include physical methods such as adsorption [6–10], coagulation and flocculation [11–15], filtration and nanofiltration [16–23] as well as biological methods [24–31]. All these methods are considered to be expensive [32] and inefficient, since the textile dyes are chemically resistant and non-biodegradable, and further treatment is required for the by-products formed and the chemicals added during the treatment process [33–36].

Advanced oxidative processes on the other hand are considered effective and innovative treatment methods for the degradation of hazardous contaminants [37]. Hydroxyl radical is the main oxidising agent formed in these processes, and it is considered the main factor responsible for complete decomposition of the organic pollutants due to its elevated oxidation potential [38–40]. These methods have been successfully approved as effective techniques for textile dye wastewater treatment [36,38,41–51]. The main products from these processes include H_2O, CO_2 and non-toxic products [45].

Advanced oxidative processes may include electrochemical oxidation [52–55], ozonation [56–58] and the Fenton process [59–61]. Electrochemical oxidation may be direct—in which the –OH group generated at the anode is the main oxidising agent—or indirect—in which chlorine and hypochlorite formed at the anode oxidise the organic contaminants.

In this work, electrochemical oxidation of methyl blue dye in sodium chloride (NaCl) electrolyte was investigated using a stainless-steel rotating cylinder anode.

* Corresponding author.

2. Experimental set-up

2.1. Materials

Samples of simulated wastewater with the desired properties were prepared with methyl blue (MB) dye, NaCl (assay 99.9%), NaOH and HCl of analytical grade purchased from the Alpha Company (India). Solution samples were prepared using distilled water, MB dye and NaCl. Solution's PH was adjusted with the aid of NaOH (0.1 N), and diluted HCl (0.1 N) solutions.

2.2. Apparatus

A 1-L glass beaker was used as the batch reactor, a 316 L stainless steel cylinder of 30 mm diameter and 50 mm length was deployed as the anode, and four carbon sheets (35 mm × 145 mm × 2 mm) were used as the cathode.

An intelligent control adjustable DC power supply (DP3003, China) was used to apply the desired value of current with the aid of two digital multimeters connected between the reactor and the power supply in order to monitor the applied current and the voltage.

A digital overhead stirrer with LED tachometer was used to move the anode at the desired rotation rate.

800 mL of simulated wastewater solutions with the required dye concentrations were added to the reactor in each run, and samples of the treated water were taken and analysed at the end of each run. The dye concentration in these samples were measured using the Shimadzu UV-1900 Spectrophotometer (Japan) at 735 nm wavelength. A plot of the experimental set-up is illustrated by Fig. 1.

3. Experimental design

A rotatable central composite design (CCD) with half factorial method was used to design the experiments in this study and obtain a mathematical model for the correlation among the removal efficiency (response) and the studied variables (estimators), with the aid of Minitab 19, by using five factors – NaCl concentration, applied current, MB concentration, rotating cylinder speed and reaction time.

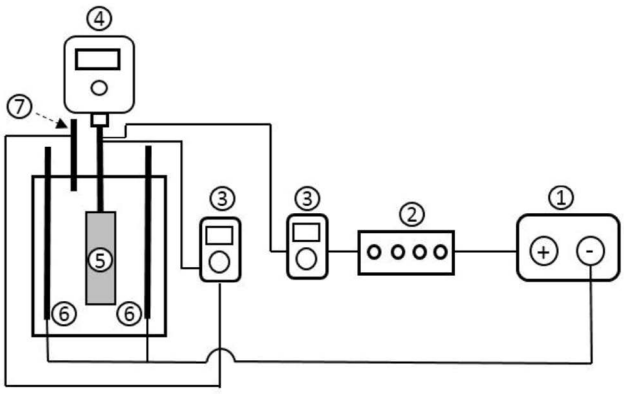

Fig. 1. Schematic diagram of experimental set-up. (1) DC power supply, (2) Resistance box, (3) Multimeter, (4) Electrical motors, (5) Stainless steel rotating cylinder anode, (6) Carbon plates cathode, (7) Reference electrode.

A set of 32 experiments were performed with one base block, six centre points in cube, 10 axial points, 16 cube points, significance level of 0.05 and with α = 2. The independent variables (predictors) utilised in this work included the initial concentration of MB (X_1), applied current (X_2), electrode rotation rate (X_3), molarity of supporting electrolyte (X_4) and reaction time (X_5). The dependent variable (response) was the removal percentage of the MB dye. The minimum and maximum values of the independent variables are shown in Table 1.

4. Results and discussion

4.1. Mathematical model

The quadratic model that establishes the correlation among the removal percentage and the independent variables used in this study was predicted by conducting and analysing the experiments according to the CCD method using the values shown in Table 2.

The obtained quadratic model has the R^2 value of 95.82%, the adjusted R^2 value of 88.22% and lack-of-fit p-value of 0.116, implying that the model is well-matched with the experimental data. This model is shown in Eq. (1).

$$\begin{aligned} Y = {} & -80.5 - 0.031X_1 + 1.050X_2 + 0.138X_3 \\ & - 6.5X_4 + 4.045X_5 - 0.001041X_1^2 \\ & - 0.001757X_2^2 - 0.000010X_3^2 + 4.44X_4^2 \\ & - 0.0423X_5^2 + 0.000193X_1X_2 - 0.000389X_1X_3 \\ & + 0.1205X_1X_4 + 0.00459X_1X_5 - 0.000204X_2X_3 \\ & - 0.1445X_2X_4 - 0.00547X_2X_5 + 0.0124X_3X_4 \\ & - 0.00223X_3X_5 + 0.106X_4X_5 \end{aligned} \quad (1)$$

The accuracy of this model can be further confirmed by plotting the predicted removal values vs. the observed removal values. The residual plot values of the response are shown in Figs. 2–6.

The normal probability of the residual plot is shown in Fig. 3a. The points in this figure are close to the straight line, with the Anderson Darling test p-value equal to 0.263. This implies that the data is normally distributed and departure from normality is insignificant, thus confirming the accuracy of the predicted model.

Table 1
Minimum and maximum values of independent variables

Coded variable	Variable name	Minimum value	Maximum value
X_1	Initial concentration of methyl blue	57	150
X_2	Applied current	80	180
X_3	Rotation rate	100	230
X_4	Molarity of supporting electrolyte	0.65	1.5
X_5	Time	16	38

Table 2
Central composite design of experiment with removal percentage values

Run order	Coded variables					Natural variables					% Removal
	X_1	X_2	X_3	X_4	X_5	X_1	X_2	X_3	X_4	X_5	
1	0	–2	0	0	0	103.5	30	165	1.075	27	34.299
2	1	1	1	–1	–1	150	180	230	0.65	16	73.333
3	0	0	0	0	0	103.5	130	165	1.075	27	90.338
4	–1	–1	–1	–1	1	57	80	100	0.65	38	73.684
5	1	–1	1	–1	1	150	80	230	0.65	38	66.666
6	0	0	0	0	0	103.5	130	165	1.075	27	84.541
7	–2	0	0	0	0	10.5	130	165	1.075	27	71.428
8	1	1	–1	–1	1	150	180	100	0.65	38	97.333
9	0	0	–2	0	0	103.5	130	35	1.075	27	79.71
10	0	0	0	0	–2	103.5	130	165	1.075	5	27.536
11	0	0	0	0	0	103.5	130	165	1.075	27	85.507
12	0	2	0	0	0	103.5	230	165	1.075	27	97.101
13	–1	1	–1	–1	–1	57	180	100	0.65	16	84.21
14	1	–1	–1	1	1	150	80	100	1.5	38	84
15	–1	–1	1	–1	–1	57	80	230	0.65	16	54.385
16	2	0	0	0	0	196.5	130	165	1.075	27	77.099
17	0	0	0	–2	0	103.5	130	165	0.225	27	89.371
18	1	1	1	1	1	150	180	230	1.5	38	96
19	1	–1	–1	–1	–1	150	80	100	0.65	16	32
20	1	1	–1	1	–1	150	180	100	1.5	16	72.666
21	0	0	0	2	0	103.5	130	165	1.925	27	83.574
22	0	0	2	0	0	103.5	130	295	1.075	27	86.473
23	1	–1	1	1	–1	150	80	230	1.5	16	50
24	0	0	0	0	0	103.5	130	165	1.075	27	86.473
25	–1	1	1	–1	1	57	180	230	0.65	38	99.5
26	0	0	0	0	2	103.5	130	165	1.075	49	98.067
27	–1	1	–1	1	1	57	180	100	1.5	38	92.982
28	–1	1	1	1	–1	57	180	230	1.5	16	82.456
29	0	0	0	0	0	103.5	130	165	1.075	27	87.439
30	–1	–1	1	1	1	57	80	230	1.5	38	82.456
31	0	0	0	0	0	103.5	130	165	1.075	27	76.811
32	–1	–1	–1	1	–1	57	80	100	1.5	16	49.122

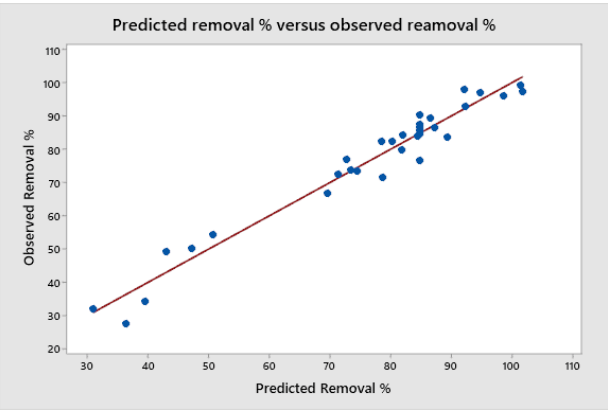

Fig. 2. Predicted vs. observed removal percentages.

The residual vs. fits plot is visualised in Fig. 3b. The figure shows that the data are randomly distributed without any particular pattern, implying that the data have a constant variance. This in turn confirms the accuracy of the predicted model.

Fig. 3d shows the residual vs. order plot. From this plot, it can be concluded whether the variables are correlated with each other or not. The random distribution without a particular pattern of data in this figure confirms that the variables are uncorrelated with each other, meaning that the predicted model is accurate.

The significancy of the standardised effect level of each variable on the removal percentage can be illustrated and compared using a Pareto chart (Fig. 4).

Fig. 4 shows that the independent variables affect the removal percentage in a descending order as per the

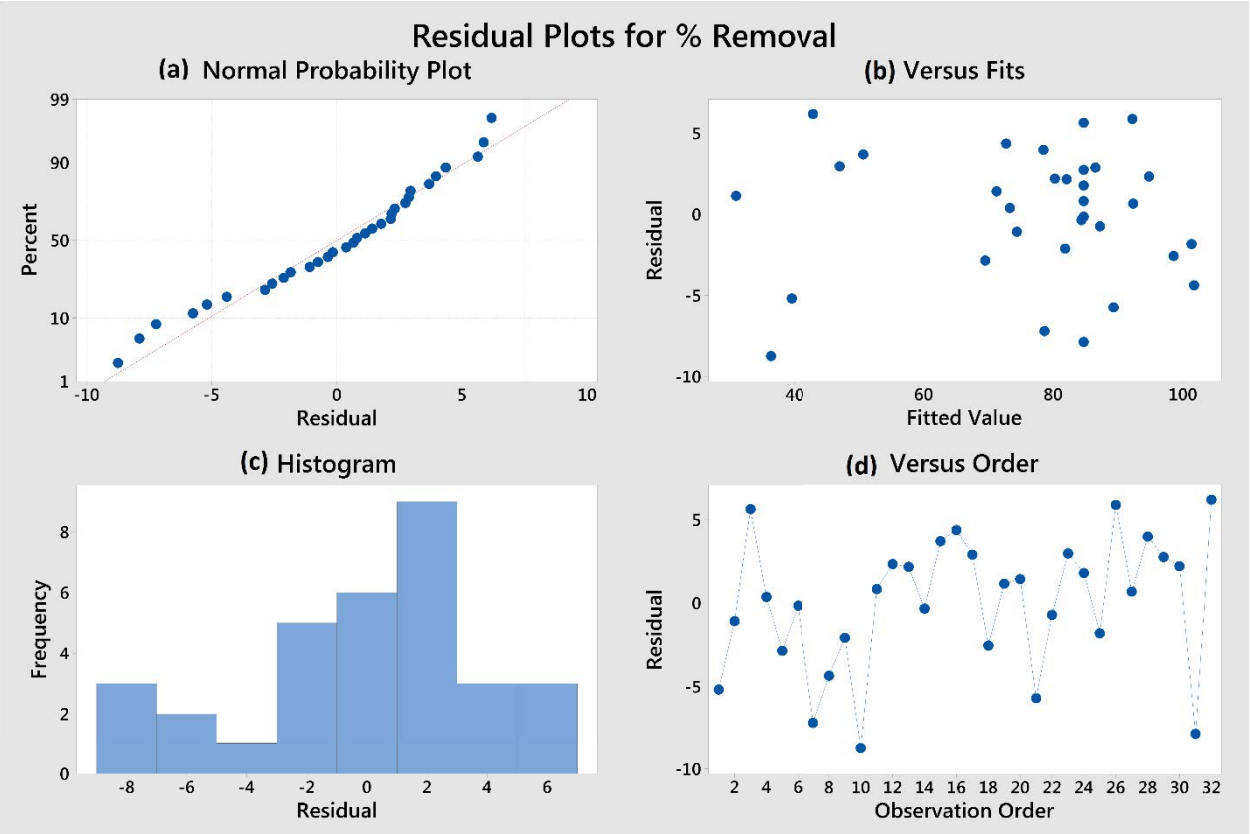

Fig. 3. Residual plots for % removal (a) normal probability plot, (b) vs. fits plot, (c) histogram plot, and (d) vs. order plot.

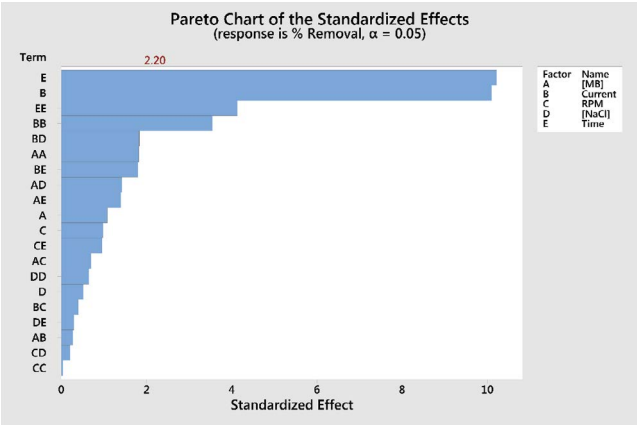

Fig. 4. Pareto chart of the standardised effects.

following sequence: time, applied current, anode rotation rate and NaCl concentration.

Effects of the studied independent variables on the MB removal percentage (response); are shown in the main effects plot of these variables (Fig. 5). It is shown that the increase in MB concentration within a certain range enhanced the removal percentage. However, after that range, any further increase in MB concentration will negatively affects the removal percentage.

Increasing the applied current to a certain extent enhanced the removal percentage. Then this percentage decreased with any further increase in the applied current. Also, the rotation rate had a positive linear effect on the removal percentage all through the applied range.

The removal percentage slightly decreased with increase in the molarity of the supporting electrolyte to a particular point, and after that it increased with elevation in molarity. Reaction time is positively affects the removal percentage to some extent, after which the removal percentage seemed to be minimised.

The interactions among the experimental variables as well as the effects of these interactions on the response are shown in Fig. 6.

4.2. Effect of initial MB concentration

Increasing the initial concentration of MB within the range of 10–94 mg/L was found to enhance the removal percentage, due to enhancement in mass transfer rate and mass transfer coefficient. This was a result of the increase in the concentration gradient between the bulk concentration and the electrode surface's concentration.

At concentrations above 94 ppm, the removal percentage was reduced with any further enhancement in concentration when the quantity of active oxidation agents (active chlorine) became insufficient to oxidise the entire lot of dye

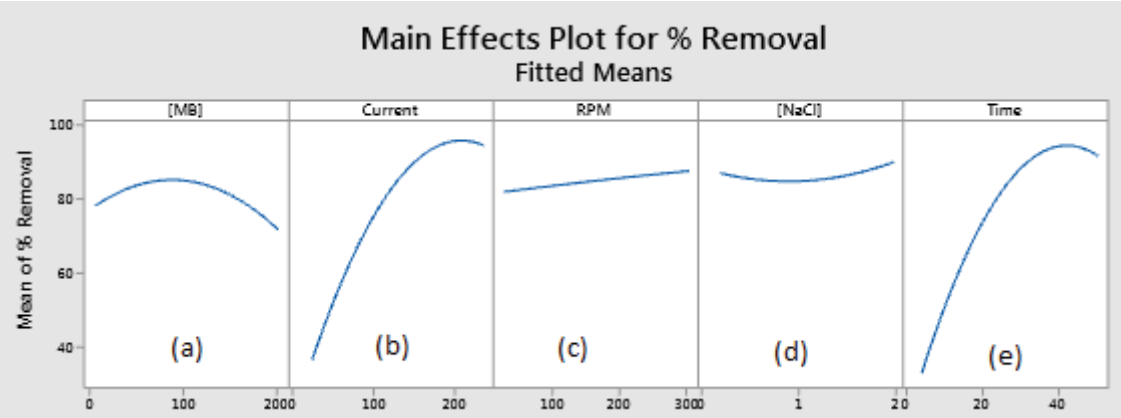

Fig. 5. Main effects of the independent variables on the removal percentage: (a) effect of methyl blue concentration, (b) effect of applied current, (c) effect of rotation rate, (d) effect of NaCl concentration, and (e) effect of reaction time.

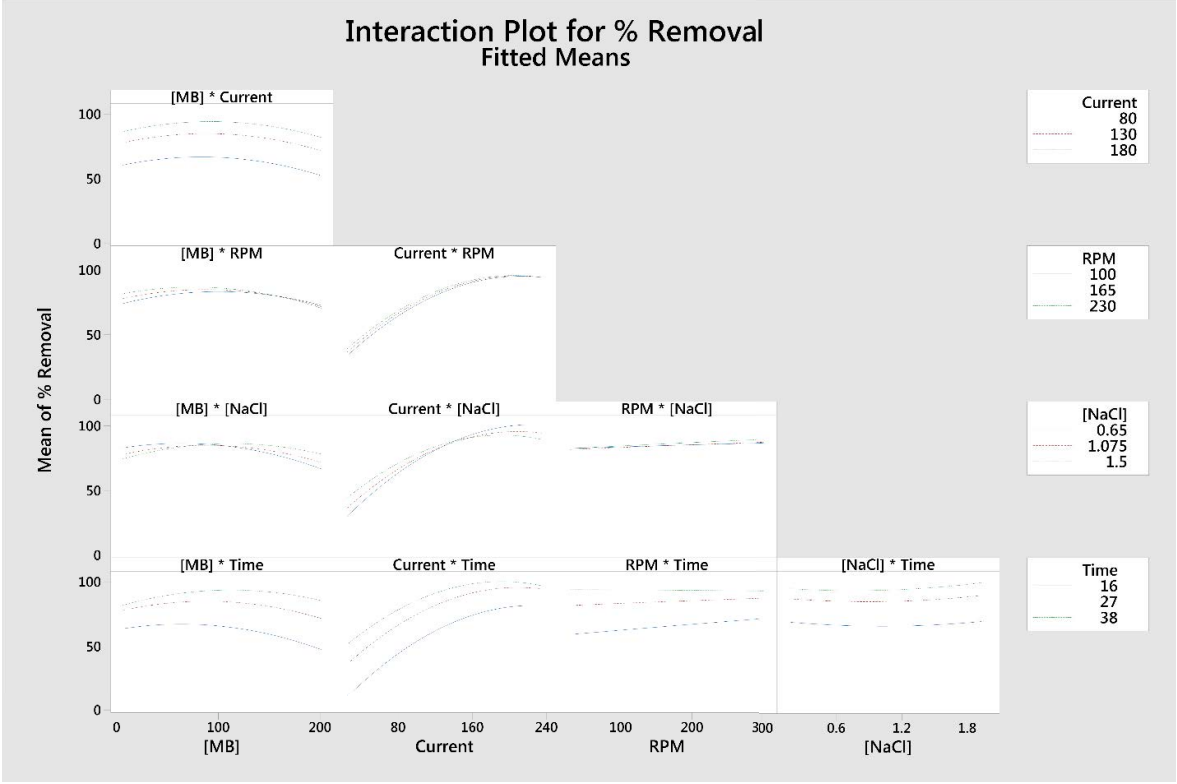

Fig. 6. Effect of the interactions among the independent variables on the removal percentage.

molecules. This resulted in a lower removal percentage. This effect is represented in Fig. 5a.

4.3. Effect of applied current

The removal percentage was significantly promoted with increase in the applied current due to increase in the amount of the oxidising agent formed (chlorine), which in turn enhanced the decomposition rate.

At 210 mA, the oxidation process reached a near-equilibrium state, and after 218 mA, the removal percentage curve showed a slight descent. This behaviour was attributable to the increase in the formation of carbon molecules resulting from the incineration reaction, which in turn affected the reading of the UV-visible instrument, causing a slight virtual reduction in the actual reading. This effect is shown in Fig. 5b.

4.4. Effect of electrode rotation rate

The electrode rotation rate significantly enhances the removal percentage through all the ranges deployed in this

work. This was attributable to the increase in mass transfer rate as a result of the mass transfer coefficient enhancement and the reduction in diffusion layer thickness formed at the anode, which enhanced the transfer of dye molecules to the surface of the electrode. This effect is illustrated in Fig. 5c.

4.5. Effect of NaCl concentration

From the predicted model, it is clear that the molarity of the supporting electrolyte is negatively affects MB removal percentage in the range of 0.2–0.88 M; then it is positively affects MB removal percentage at molarity values higher than 0.88.

It is thought that the degradation mechanism is direct oxidation in the range of 0.2–0.88 M, and that an increase in molarity through this range will reduce the removal percentage, due to the increase in viscosity and as a result of salt film formation at the electrode surface. This in turn inhibits electrons' transfer at the interface between the solution and electrode.

For molarity values higher than 0.88, the degradation mechanism is thought to be indirect, and hence, an increase in the NaCl concentration will increase the chances of active chlorine formation as a strong oxidising agent, leading to a higher removal percentage. This effect is shown in Fig. 5d.

4.6. Effect of time

The removal percentage increased significantly with time due to the seemingly quick incineration reaction rate during the first 35 min of the reaction, since the reaction rate is proportional to the initial concentration of the reactants. However, after 35 min, the reaction rate became slow due to depletion in the number of molecules of the oxidising agents. The effect of the reaction time is shown in Fig. 5e.

5. Process optimisation

The response surface methodology is an effective statistical design for mathematical model prediction and data analysis, while the CCD is an effective method for optimising independent variables (predictors) and obtaining an optimum response.

The interactions among operating variables and their effects on the removal percentage are illustrated through contour and surface plots of removal percentage, shown in Figs. 7 and 8.

This figure shows that the optimum (highest) removal percentage exists within the region confined by 156–228 mA applied current and 21–170 mg/L dye concentration.

The optimum conditions were determined according to these figures, while the optimisation procedure was performed according to the settings illustrated in Table 3.

The optimum conditions required to obtain the optimum response (maximum removal % of 99.5%) are shown in Table 4.

The optimisation plot of the maximum removal percentage with the highest, lowest and optimum values of independent variables is shown in Fig. 9.

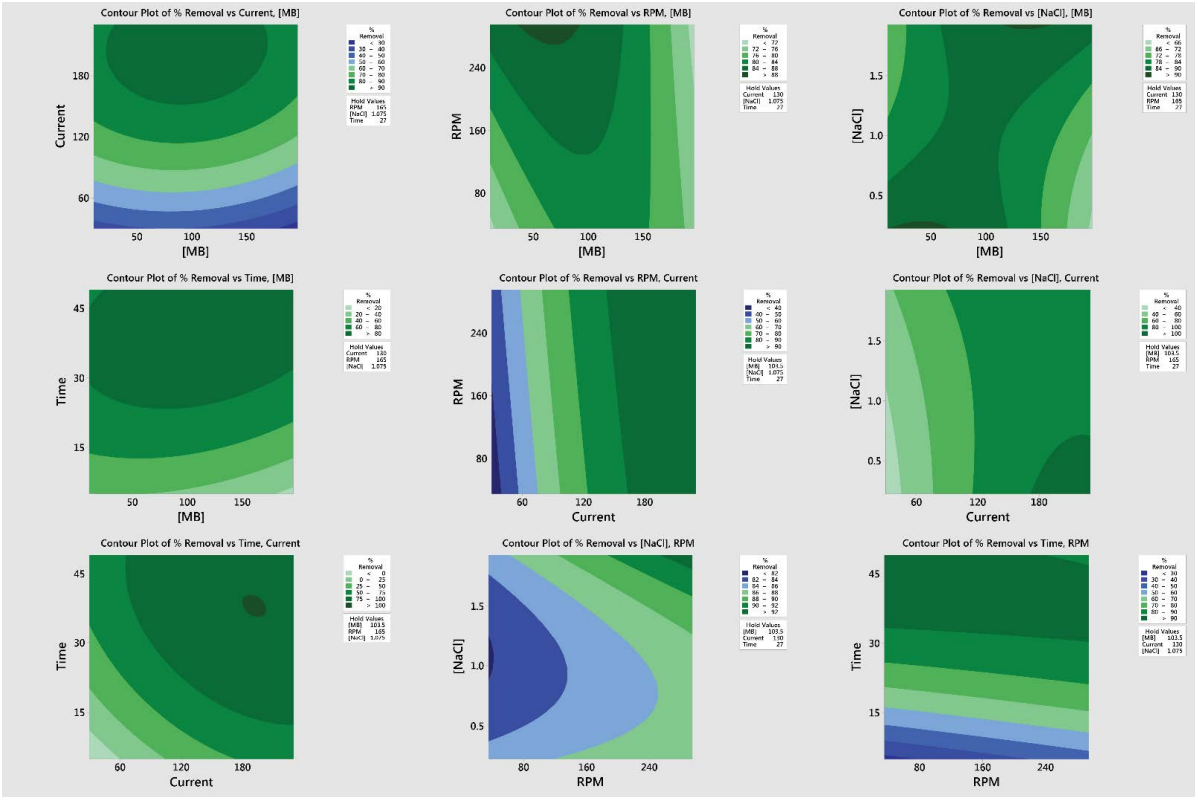

Fig. 7. Contour plot of methyl blue removal percentage vs. applied variables.

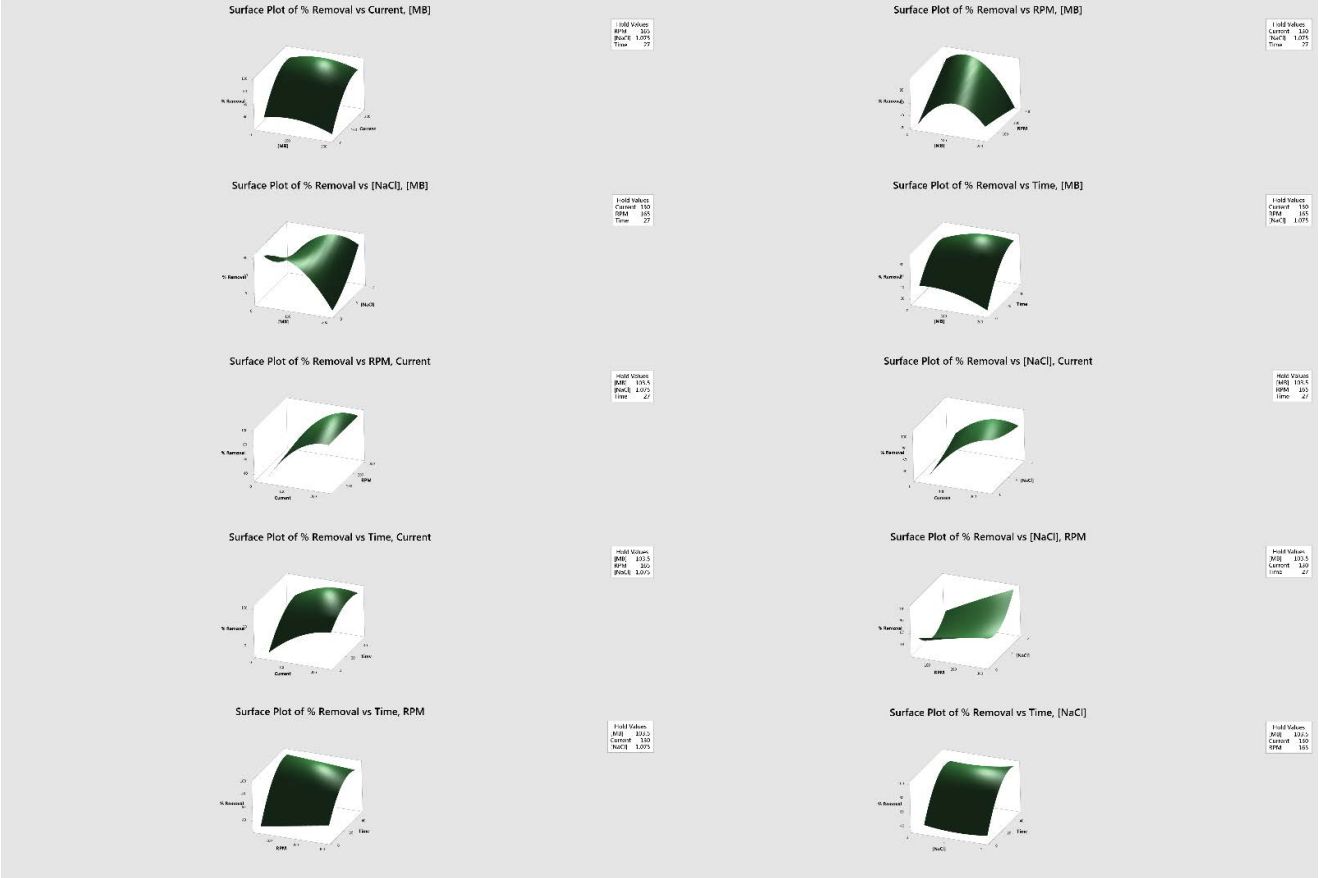

Fig. 8. Surface plot of removal percentage vs. applied variables.

Table 3
Optimisation parameter settings

Response	% Removal
Goal	Maximum
Lower	27.536
Target	99.5
Upper weight	1
Importance	1

Table 4
Optimum conditions

Solution	1
[MB]	95.0455
Current	230
rpm	35
[NaCl]	0.225
Time	37.4444
% Removal fit	115.113
Composite desirability	1

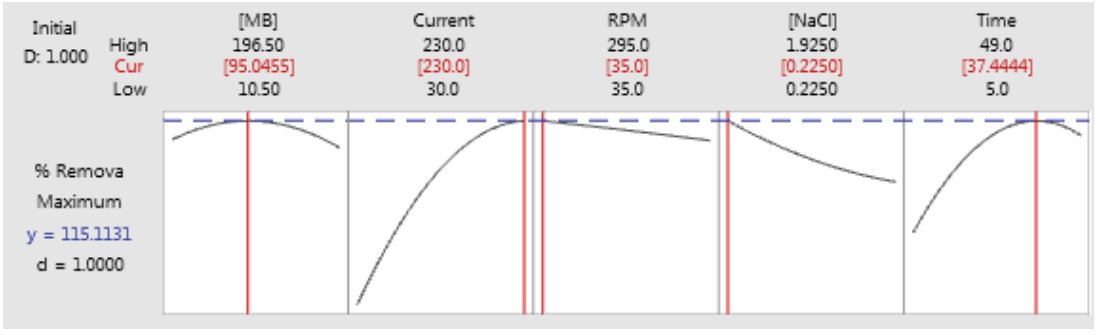

Fig. 9. Optimisation plot of maximum removal percentage.

6. Conclusions

In this study, the electrochemical removal of MB dye from simulated wastewater was investigated, and the removal percentage was correlated with the operating variables by a full quadratic regression correlation. Furthermore, the effect of individual variables on the response were studied and the optimum conditions were determined. The conclusions were as follows:

- The MB dye can be successfully removed by electrochemical oxidation with the rotating cylinder electrode.
- The mathematical model among the removal percentage and the operating variables was predicted and tested for accuracy with the aid of the response surface methodology and the CCD of the experiments.
- MB concentration is positively affects MB removal percentage through the range of 10–94 mg/L, and negatively affects MB removal percentage for dye concentrations higher than 94 mg/L.
- Generally, the applied current has a positive effect on the dye decomposition, and this effect reaches an equilibrium state at 210 mA.
- Increasing the anode's rotation rate will significantly enhance the removal percentage over the entire applied range of the anode rotation rate.
- The removal percentage significantly increased with time during the first 35 min and then the incineration reaction turned slower.
- The dye degradation occurred by direct oxidation within the range of 0.2–0.88 M NaCl with negative effect of NaCl molarity, and by indirect oxidation at NaCl molarity levels higher than 0.88 with positive effect of NaCl molarity.
- The optimum conditions for the highest removal percentage (99.5%) were 95.0455 mg/L MB concentration, 230 mA applied current, 35 rpm, 0.255 M supporting electrolyte and reaction time of 37.444 min.

References

[1] P. Kaur, V.K. Sangal, J.P. Kushwaha, Modeling and evaluation of electro-oxidation of dye wastewater using artificial neural networks, RSC Adv., 5 (2015) 34663–34671.

[2] D. Stergiopoulos, K. Dermentzis, P. Giannakoudakis, S. Sotiropoulos, Electrochemical decolorization and removal of indigo carmine textile dye from wastewater, Global Nest J., 16 (2014) 499–506.

[3] C. Gutiérrez-Bouzán, M. Pepió, Interaction between pH and conductivity in the indirect electro-oxidation of azo dyes, Ind. Eng. Chem. Res., 53 (2014) 18993–19000.

[4] F.J. Recio, P. Herrasti, I. Sirés, A.N. Kulak, D.V. Bavykin, C. Ponce-de-León, F.C. Walsh, The preparation of PbO_2 coatings on reticulated vitreous carbon for the electro-oxidation of organic pollutants, Electrochim. Acta, 56 (2011) 5158–5165.

[5] S. Khezrianjoo, H.D. Revanasiddappa, Evaluation of kinetics and energy consumption of the electrochemical oxidation of Acid Red 73 in aqueous media, Toxicol. Environ. Chem., 2248 (2016) 23–41.

[6] A.Z. Bouyakoub, B.S. Lartiges, R. Ouhib, S. Kacha, A.G. El Samrani, J. Ghanbaja, O. Barres, $MnCl_2$ and $MgCl_2$ for the removal of reactive dye Levafix Brilliant Blue EBRA from synthetic textile wastewaters: an adsorption/aggregation mechanism, J. Hazard. Mater., 187 (2011) 264–273.

[7] T. Fazal, A. Razzaq, F. Javed, A. Hafeez, N. Rashid, U.S. Amjad, M.S. Ur Rehman, A. Faisal, F. Rehman, Integrating adsorption and photocatalysis: a cost effective strategy for textile wastewater treatment using hybrid biochar-TiO_2 composite, J. Hazard. Mater., 390 (2020) 121623, doi: 10.1016/j.jhazmat.2019.121623.

[8] H. Patel, Charcoal as an adsorbent for textile wastewater treatment, Sep. Sci. Technol., 53 (2018) 2797–2812.

[9] K. Yang, Y. Liu, Y. Li, Z. Cao, C. Zhou, Z. Wang, X. Zhou, S.A. Baig, X. Xu, Applications and characteristics of Fe-Mn binary oxides for Sb(V) removal in textile wastewater: Selective adsorption and the fixed-bed column study, Chemosphere, 232 (2019) 254–263.

[10] M.H. Alhassani, S.M. Al-Jubouri, H.A. Al-Jendeel, Stabilization of phenol trapped by agricultural waste: a study of the influence of ambient temperature on the adsorbed phenol, Desal. Water Treat., 187 (2020) 266–276.

[11] M. Riera-Torres, C. Gutiérrez-Bouzán, M. Crespi, Combination of coagulation–flocculation and nanofiltration techniques for dye removal and water reuse in textile effluents, Desalination, 252 (2010) 53–59.

[12] J. Dotto, M.R. Fagundes-Klen, M.T. Veit, S.M. Palácio, R. Bergamasco, Performance of different coagulants in the coagulation/flocculation process of textile wastewater, J. Cleaner Prod., 208 (2019) 656–665.

[13] F. Harrelkas, A. Azizi, A. Yaacoubi, A. Benhammou, M. Noelle Pons, Treatment of textile dye effluents using coagulation–flocculation coupled with membrane processes or adsorption on powdered activated carbon, Desalination, 235 (2009) 330–339.

[14] B. Keskin, M.E. Ersahin, H. Ozgun, I. Koyuncu, Pilot and full-scale applications of membrane processes for textile wastewater treatment: a critical review, J. Water Process Eng., 42 (2021) 102172, doi: 10.1016/j.jwpe.2021.102172.

[15] C.S.D. Rodrigues, L.M. Madeira, R.A.R. Boaventura, Treatment of textile dye wastewaters using ferrous sulphate in a chemical coagulation/flocculation process, Environ. Technol., 34 (2013) 719–729.

[16] E. Debik, G. Kaykioglu, A. Coban, I. Koyuncu, Reuse of anaerobically and aerobically pre-treated textile wastewater by UF and NF membranes, Desalination, 256 (2010) 174–180.

[17] E. Ellouze, N. Tahri, R. Ben Amar, Enhancement of textile wastewater treatment process using nanofiltration, Desalination, 286 (2012) 16–23.

[18] F.M. Gunawan, D. Mangindaan, K. Khoiruddin, I. Gede Wenten, Nanofiltration membrane cross-linked by *m*-phenylenediamine for dye removal from textile wastewater, Polym. Adv. Technol., 30 (2019) 360–367.

[19] D. Ji, C. Xiao, S. An, J. Zhao, J. Hao, K. Chen, Preparation of high-flux PSF/GO loose nanofiltration hollow fiber membranes with dense-loose structure for treating textile wastewater, Chem. Eng. J., 363 (2019) 33–42.

[20] J. Korenak, C. Hélix-nielsen, H. Bukšek, I. Petrinić, Efficiency and economic feasibility of forward osmosis in textile wastewater treatment, J. Cleaner Prod., 210 (2019) 1483–1495.

[21] E. Kurt, D.Y. Koseoglu-Imer, N. Dizge, S. Chellam, I. Koyuncu, Pilot-scale evaluation of nanofiltration and reverse osmosis for process reuse of segregated textile dyewash wastewater, Desalination, 302 (2012) 24–32.

[22] Y.K. Ong, F.Y. Li, S.-P. Sun, B.-W. Zhao, C.-Z. Liang, T.-S. Chung, Nanofiltration hollow fiber membranes for textile wastewater treatment: lab-scale and pilot-scale studies, Chem. Eng. Sci., 114 (2014) 51–57.

[23] S.-Y. Wang, Y.-F. Chen, H. Zhou, X.-H. Xu, L.-H. Cheng, Calcium carbonate scaling in forward osmosis for textile reverse osmosis concentrate treatment, J. Water Process Eng., 35 (2020) 101181, doi: 10.1016/j.jwpe.2020.101181.

[24] Q. Chen, Y. Yang, M. Zhou, M. Liu, S. Yu, C. Gao, Comparative study on the treatment of raw and biologically treated textile effluents through submerged nanofiltration, J. Hazard. Mater., 284 (2015) 121–129.

[25] S. Mishra, J.K. Nayak, A. Maiti, Bacteria-mediated biodegradation of reactive azo dyes coupled with bio-energy generation from model wastewater, Clean Technol. Environ. Policy, 22 (2020) 651–667.

[26] A. Paz, J. Carballo, M.J. Pérez, J.M. Domínguez, Biological treatment of model dyes and textile wastewaters, Chemosphere, 181 (2017) 168–177.
[27] S. Popli, U.D. Patel, Destruction of azo dyes by anaerobic–aerobic sequential biological treatment: a review, Int. J. Environ. Sci. Technol., 12 (2015) 405–420.
[28] M. Punzi, A. Anbalagan, R. Aragão Börner, B.-M. Svensson, M. Jonstrup, B. Mattiasson, Degradation of a textile azo dye using biological treatment followed by photo-Fenton oxidation: evaluation of toxicity and microbial community structure, Chem. Eng. J., 270 (2015) 290–299.
[29] R. Shoukat, S.J. Khan, Y. Jamal, Hybrid anaerobic-aerobic biological treatment for real textile wastewater, J. Water Process Eng., 29 (2019) 100804, doi: 10.1016/j.jwpe.2019.100804.
[30] M. Concetta Tomei, J. Soria Pascual, D. Mosca Angelucci, Analysing performance of real textile wastewater bio-decolourization under different reaction environments, J. Cleaner Prod., 129 (2016) 468–477.
[31] H. Xu, B. Yang, Y. Liu, F. Li, C. Shen, C. Ma, Q. Tian, X. Song, W. Sand, Recent advances in anaerobic biological processes for textile printing and dyeing wastewater treatment: a mini-review, World J. Microbiol. Biotechnol., 34 (2018) 165, doi: 10.1007/s11274-018-2548-y.
[32] Z. Liu, F. Wang, Y. Li, T. Xu, S. Zhu, Continuous electrochemical oxidation of methyl orange waste water using a three-dimensional electrode reactor, J. Environ. Sci., 23 (2011) S70–S73.
[33] D. Suteu, D. Bilba, Equilibrium and kinetic study of Reactive Dye Brilliant Red HE-3B adsorption by activated charcoal, Acta Chim. Slov., 52 (2005) 73–79.
[34] E. Guivarch, S. Trevin, C. Lahitte, M.A. Oturan, Degradation of azo dyes in water by electro-Fenton process, Environ. Chem. Lett., 1 (2003) 38–44.
[35] S. Raghu, C. Woo Lee, S. Chellammal, S. Palanichamy, C. Ahmed Basha, Evaluation of electrochemical oxidation techniques for degradation of dye effluents—a comparative approach, J. Hazard. Mater., 171 (2009) 748–754.
[36] A.A.P. Mansur, H.S. Mansur, F.P. Ramanery, L.C. Oliveira, P.P. Souza, "Green" colloidal ZnS quantum dots/chitosan nano-photocatalysts for advanced oxidation processes: study of the photodegradation of organic dye pollutants, Appl. Catal., B, 158–159 (2014) 269–279.
[37] B.L. Alderete, J. da Silva, R. Godoi, F.R. da Silva, S.R. Taffarel, L.P. da Silva, A.L.H. Garcia, H. Mitteregger Júnior, H.L.N. de Amorim, J.N. Picada, Evaluation of toxicity and mutagenicity of a synthetic effluent containing azo dye after advanced oxidation process treatment, Chemosphere, 263 (2021) 128291, doi: 10.1016/j.chemosphere.2020.128291.
[38] S. Chakma, L. Das, V.S. Moholkar, Dye decolorization with hybrid advanced oxidation processes comprising sonolysis/Fenton-like/photo-ferrioxalate systems: a mechanistic investigation, Sep. Purif. Technol., 156 (2015) 596–607.
[39] D. Syam Babu, V. Srivastava, P.V. Nidheesh, M. Suresh Kumar, Detoxification of water and wastewater by advanced oxidation processes, Sci. Total Environ., 696 (2019) 133961, doi: 10.1016/j.scitotenv.2019.133961.
[40] R. Arshad, T.H. Bokhari, T. Javed, I.A. Bhatti, S. Rasheed, M. Iqbal, A. Nazir, S. Naz, M.I. Khan, M.K.K. Khosa, M. Iqbal, M. Zia-ur-Rehman, Degradation product distribution of Reactive Red-147 dye treated by UV/H_2O_2/TiO_2 advanced oxidation process, J. Mater. Res. Technol., 9 (2020) 3168–3178.
[41] H. Lee, Y.-K. Park, S.-J. Kim, B.-H. Kim, H.-S. Yoon, S.-C. Jung, Rapid degradation of methyl orange using hybrid advanced oxidation process and its synergistic effect, J. Ind. Eng. Chem., 35 (2016) 205–210.
[42] M. Faouzi, P. Cañizares, A. Gadri, J. Lobato, B. Nasr, R. Paz, M.A. Rodrigo, C. Saez, Advanced oxidation processes for the treatment of wastes polluted with azoic dyes, Electrochim. Acta, 52 (2006) 325–331.
[43] S.H.S. Chan, T.Y. Wu, J.C. Juan, C.Y. Teh, Recent developments of metal oxide semiconductors as photocatalysts in advanced oxidation processes (AOPs) for treatment of dye waste-water, J. Chem. Technol. Biotechnol., 86 (2011) 1130–1158.
[44] J.R. Guimarães, M. Guedes Maniero, R. Nogueira de Araújo, A comparative study on the degradation of RB-19 dye in an aqueous medium by advanced oxidation processes, J. Environ. Manage., 110 (2012) 33–39.
[45] A. Zuorro, R. Lavecchia, Evaluation of UV/H_2O_2 advanced oxidation process (AOP) for the degradation of diazo dye Reactive Green 19 in aqueous solution, Desal. Water Treat., 52 (2014) 1571–1577.
[46] A. Thiam, E. Brillas, J.A. Garrido, R.M. Rodríguez, I. Sirés, Routes for the electrochemical degradation of the artificial food azo-colour Ponceau 4R by advanced oxidation processes, Appl. Catal., B, 180 (2016) 227–236.
[47] M.A. Hassaan, A. El Nemr, F.F. Madkour, Testing the advanced oxidation processes on the degradation of Direct Blue 86 dye in wastewater, Egypt. J. Aquat. Res., 43 (2017) 11–19.
[48] J. Paul Guin, Y.K. Bhardwaj, L. Varshney, Mineralization and biodegradability enhancement of Methyl Orange dye by an effective advanced oxidation process, Appl. Radiat. Isot., 122 (2017) 153–157.
[49] S. Alcocer, A. Picos, A.R. Uribe, T. Pérez, J.M. Peralta-Hernández, Comparative study for degradation of industrial dyes by electrochemical advanced oxidation processes with BDD anode in a laboratory stirred tank reactor, Chemosphere, 205 (2018) 682–689.
[50] G.G. Bessegato, J.C. de Souza, J.C. Cardoso, M.V.B. Zanoni, Assessment of several advanced oxidation processes applied in the treatment of environmental concern constituents from a real hair dye wastewater, J. Environ. Chem. Eng., 6 (2018) 2794–2802.
[51] P.V. Nidheesh, M. Zhou, M.A. Oturan, An overview on the removal of synthetic dyes from water by electrochemical advanced oxidation processes, Chemosphere, 197 (2018) 210–227.
[52] S. Singh, S.L. Lo, V.C. Srivastava, A.D. Hiwarkar, Comparative study of electrochemical oxidation for dye degradation: parametric optimization and mechanism identification, J. Environ. Chem. Eng., 4 (2016) 2911–2921.
[53] V.M. Vasconcelos, F.L. Migliorini, J.R. Steter, M.R. Baldan, N.G. Ferreira, M.R. de Vasconcelos Lanza, Electrochemical oxidation of RB-19 dye using a highly BDD/Ti: proposed pathway and toxicity, J. Environ. Chem. Eng., 4 (2016) 3900–3909.
[54] I.M. Sasidharan Pillai, A.K. Gupta, Performance analysis of a continuous serpentine flow reactor for electrochemical oxidation of synthetic and real textile wastewater: energy consumption, mass transfer coefficient and economic analysis, J. Environ. Manage., 193 (2017) 524–531.
[55] J. Zou, X. Peng, M. Li, Y. Xiong, B. Wang, F. Dong, B. Wang, Electrochemical oxidation of COD from real textile wastewaters: kinetic study and energy consumption, Chemosphere, 171 (2017) 332–338.
[56] S. Ledakowicz, R. Żyłła, K. Paździor, J. Wrębiak, J. Sójka-Ledakowicz, Integration of ozonation and biological treatment of industrial wastewater from dyehouse, Ozone Sci. Eng., 39 (2017) 357–365.
[57] S.P. Ghuge, A.K. Saroha, Catalytic ozonation of dye industry effluent using mesoporous bimetallic Ru-Cu/SBA-15 catalyst, Process Saf. Environ. Prot., 118 (2018) 125–132.
[58] A. Muniyasamy, G. Sivaporul, A. Gopinath, R. Lakshmanan, A. Altaee, A. Achary, P.V. Chellam, Process development for the degradation of textile azo dyes (mono-, di-, poly-) by advanced oxidation process - ozonation: experimental & partial derivative modelling approach, J. Environ. Manage., 265 (2020) 110397, doi: 10.1016/j.jenvman.2020.110397.
[59] S.K. Patel, S.G. Patel, G.V. Patel, Degradation of reactive dye in aqueous solution by fenton, photo-Fenton process and combination process with activated charcoal and TiO_2, Proc. Natl. Acad. Sci., India, Sect. A Phys. Sci., 90 (2020) 579–591.
[60] V. Kumar, D. Ghime, P. Ghosh, Decolorization of textile dye Rifafix Red 3BN by natural hematite and a comparative study on different types of Fenton process, Chem. Eng. Commun., 207 (2020) 1380–1389.
[61] E. Baştürk, A. Alver, Modeling azo dye removal by sono-fenton processes using response surface methodology and artificial neural network approaches, J. Environ. Manage., 248 (2019) 109300, doi: 10.1016/j.jenvman.2019.109300.